Aging alters envelope representations of speech-like sounds in the inferior colliculus

Aravindakshan Parthasarathy[1,2,#], Björn Herrmann[3,#], Edward L. Bartlett[1*]

[1] Depts. of Biological Sciences and Biomedical Engineering, Purdue University,
West Lafayette, IN, 47906, USA

[2] Dept. of Otolaryngology, Harvard Medical School, and Eaton-Peabody Laboratories,
Massachusetts Eye and Ear Infirmary, Boston, MA 02114

[3] Department of Psychology & Brain and Mind Institute, The University of Western Ontario,
London, ON, N6A 3K7, Canada

[#]Aravindakshan Parthasarathy and Björn Herrmann contributed equally to this work.

*Correspondence concerning this article should be addressed to Edward L Bartlett, 206 S. Martin Jischke Drive, West Lafayette, IN - 47906. E-mail: ebartle@purdue.edu

Running title: Envelope coding deficits with age in the IC

Conflict of Interest: The authors declare no competing conflicts of interest

ABSTRACT

Hearing impairment in aging is thought to arise from impaired temporal processing in auditory circuits. We used a systems-level (scalp recordings) and a microcircuit-level (extracellular recordings) approach to investigate how aging affects the sensitivity to temporal envelopes of speech-like sounds in rats. Scalp-recorded potentials suggest an age-related increase in sensitivity to temporal regularity along the ascending auditory pathway. The underlying cellular changes in the midbrain were examined using extracellular recordings from inferior colliculus neurons. We observed an age-related increase in sensitivity to the sound's onset and temporal regularity (i.e., periodicity envelope) in the spiking output of inferior colliculus neurons, relative to their synaptic inputs (local field potentials). This relative enhancement for aged animals was most prominent for multi-unit (relative to single-unit) spiking activity. Spontaneous multi-unit, but not single-unit, activity was also enhanced in aged compared to young animals. Our results suggest that aging is associated with altered sensitivity to a sound's temporal regularities, and that these effects may be due to increased gain of neural network activity in the midbrain.

Keywords: inferior colliculus, voice onset time, evoked potentials, hearing loss

INTRODUCTION

Older and middle-aged listeners experience difficulties understanding speech, particularly in challenging listening situations such as in the presence of background sounds, competing speakers, or reverberation (Ruggles et al., 2011, Pichora-Fuller and Souza, 2001). Speech perception depends on the sensitivity of the auditory system to temporal regularities in sounds. Temporal regularities in speech may be divided into three categories: the slow fluctuations (<50 Hz) of the speech envelope that capture word and syllabic rate; the periodicity envelope (50–500 Hz), which contains the fundamental frequency of the speaker's voice (f0) and is crucial for speaker identification (Bregman, 1990); and the temporal fine structure (>500 Hz), which contains information about formant structure (Rosen, 1992). The sensitivity of the auditory system to temporal regularity in sounds declines with age, with drastic consequences for speech perception (Walton, 2010, Fullgrabe et al., 2015, Anderson et al., 2011), but the neurophysiological changes that underlie this age-related decline are not well understood.

An age-related decline in temporal processing abilities is thought to be primarily neural in origin, because it is independent of changes in hearing thresholds due to impaired cochlear function (Frisina and Frisina, 1997, Pichora-Fuller and Souza, 2001, Gordon-Salant and Fitzgibbons, 2001). The neural deficits that may contribute to impaired sensitivity to temporal regularity include cochlear synaptopathy – that is, the degradation of cochlear synapses between inner hair cells and auditory nerve fibers (Sergeyenko et al., 2013) – and a decrease in inhibitory neurotransmitters in the brainstem, midbrain and cortex (Caspary et al., 2008, Takesian et. al., 2009, Rabang et al., 2012). Loss of inhibition may result in increased neural activity in central auditory regions despite diminished inputs from peripheral structures (Mohrle et al., 2016, Parthasarathy et al., 2014, Hughes et al., 2010). However, it is less clear how aging affects sensitivity to temporal regularity in central auditory regions, in particular for complex, speech-like sounds.

Previous work suggests that neurons in the inferior colliculus show altered temporal processing including changes in the sensitivity to the temporal regularities in sounds (Walton et al., 2002, Walton et

al., 1998, Palombi et al., 2001, Rabang et al., 2012, Schatteman et al., 2008). These studies focused on neuronal spiking, which reflects the output of neurons. In contrast, local field potentials (LFPs) are thought to reflect the summed synaptic inputs to a neuron or local neuronal population to a large degree (but other non-synaptic activity might additionally contribute; (Bullock, 1997, Buzsaki et al., 2012, Logothetis and Wandell, 2004, Logothetis et al., 2001)). Recent recordings of LFPs and spiking activity show that synchronization of spiking activity (output) is abnormally enhanced in the aging inferior colliculus, despite decreased synaptic inputs (input), and that this age-related relative increase in activity (i.e., from a neuron's input to its output) is specific for sounds with modulation rates below 100 Hz (Herrmann et al., 2017). Whether aging also leads to an over-sensitivity to temporal regularities in complex, speech-like sounds is unknown.

In the current study, we test the hypothesis that neural synchronization to the periodicity envelope (~100 Hz) of speech is abnormally enhanced in the inferior colliculus of aged animals. We assess peripheral neural function by measuring wave 1 amplitudes of the auditory brainstem responses (ABRs) and show physiological evidence for cochlear synaptopathy in aged animals. Scalp-recorded neural synchronization to the envelope of a speech-like stimulus is increased specifically in more rostral regions in the auditory pathway such as the inferior colliculus compared to more caudal ones such as the auditory nerve. Further, we assess the relation between LFPs (synaptic input) and spiking output in the inferior colliculus using extracellular recordings. Synchronization of LFPs to the envelope of a speech-like sound is decreased in aged animals, whereas synchronization of spiking activity from well isolated units does not differ between age groups. Multi-unit spike synchronization, however, is drastically increased for aged animals, suggesting changes in gain control mechanisms occurring largely at a neural network level.

METHODS AND MATERIALS

Ethical approval

The experimental procedures described in the present investigation were approved by the Institutional Animal Care and Use Committee of Purdue University (PACUC #1111000167). The experiments included in this study comply with the policies and regulations described by (Drummond, 2009). Rats were housed one per cage in accredited facilities (Association for the Assessment and Accreditation of Laboratory Animal Care) with food and water provided *ad libitum*. The number of animals used was reduced to the minimum necessary to allow adequate statistical analyses.

Subject population

The study design is cross-sectional and used male Fischer-344 rats obtained from Charles River Laboratories and Taconic. The aging Fisher-344 rat has been suggested to be a suitable model to study presbycusis in aging animals (Syka, 2010) and has been shown to exhibit high frequency hearing loss and metabolic presbycusis that are characteristic of human age-related loss of hearing sensitivity (Dubno et al., 2013, Allen and Eddins, 2010). 11 young (3–6 months, ~300 g) and 12 aged (22–26 months, ~400–500 g) animals were used for scalp recordings, and 11 young (3–6 months, ~300 g) and 9 aged (22–26 months, ~400–500 g) animals were used for extracellular recordings. A subset of the ABR recordings have been reported in previous studies (Parthasarathy and Bartlett, 2012, Parthasarathy et. al., 2014).

Sound stimulation

The stimulus was a natural English syllable, /ba/, which was 260ms long and spoken by a male speaker of North American English with a fundamental frequency ~110Hz. In order to account for the differences in the hearing range between rats and humans, as well as to increase the number of responsive neurons in the inferior colliculus of rats, this speech token was half-wave rectified, and used to modulate a

broadband noise carrier (0.04–40 kHz) (Figure 1A). This preserved the periodicity envelope as well as the original fine stricture of the speech token, both of which served as the modulator for the broadband noise (Figure 1B, C). This stimulus design was chosen to understand how neurons represent temporal regularities that are important for human speech and to aid comparison with human literature, rather than investigating the representation of conspecific vocalizations that may not generalize to human speech processing.

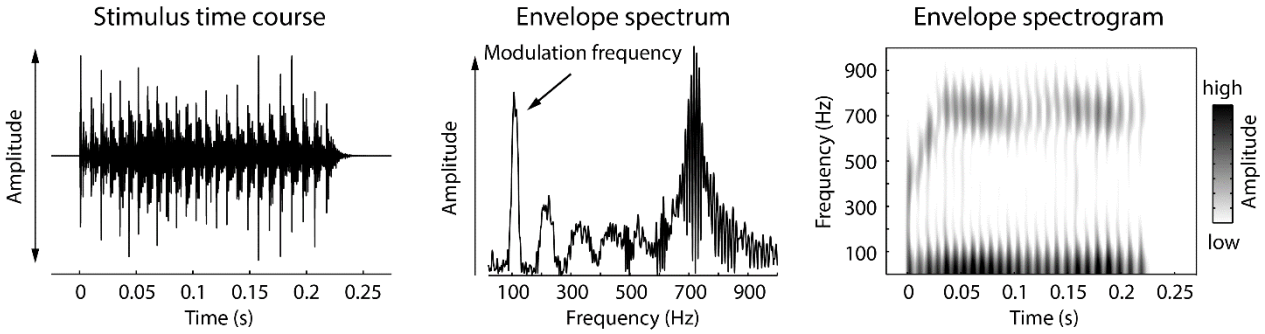

Figure 1: Speech-like sound used in the current study. Left: Waveform of the speech-like sound. **Middle:** Amplitude spectrum of the envelope of the speech-like sound displayed on the left. **Right:** Spectrogram of the envelope of the speech-like sound.

Stimulus generation

Sound stimuli were generated using SigGenRP (Tucker-Davis Technologies, TDT) sampled at a rate of 97.64 kHz (standard TDT sampling rate) and presented through custom-written interfaces in OpenEx software (TDT). Sound waveforms were generated via a multichannel processor (RX6, TDT), amplified (SA1, TDT), and presented free-field through a Bowers and Wilkins DM601 speaker. The output from the speaker was calibrated free field, using SigCal (TDT) and a Bruel Kjaer microphone with a 0.25-in. condenser, pointed at frontal incidence to the speaker, from the same location as the animal's right ear, and was found to be within ±6 dB for the frequency range tested. All recordings took place in an Industrial Acoustics booth lined with 1 inch (35 mm) Sonex foam with ~90% absorption for frequencies ≥1000 Hz,

124 minimizing potential echoes or reverberations. All analyses described below accounted for the travel
125 time of the sound wave from the speaker to the animals' ears.

126 ***Electrophysiological recordings at the scalp***

127 Methods for experimental setup, sound stimulation, and scalp-potential recordings are similar to
128 those described before (Parthasarathy et al., 2016, Parthasarathy et al., 2014). The animals were briefly
129 anesthetized using isoflurane (1.5–2%) for the insertion of subdermal needle electrodes (Ambu) and the
130 intramuscular injection of dexmedetomidine (Dexdomitor, 0.2 mg/kg), an α-adrenergic agonist that acts
131 as a sedative and an analgesic. Recordings commenced after a 15 minute recovery from the anesthesia,
132 and were terminated if the animal showed any signs of discomfort like increased breathing or major
133 movement as monitored by a video camera in the recording chamber.

134 The scalp-evoked responses to the temporal envelope of the speech-like sound (Envelope following
135 response - EFR) were obtained using two simultaneous recording channels. One positive electrode
136 (caudal channel) was placed on the animal's forehead along the midline at Cz – Fz. This electrode has a
137 strong wave 3 ABR component (cochlear nuclei) and best sensitivity to modulation frequencies ≥100 Hz
138 (Parthasarathy and Bartlett 2012). Another positive electrode (rostral channel) was placed horizontally,
139 along the inter-aural line, above the location of the inferior colliculus. This electrode has a strong wave
140 1, 4 and 5 ABR components (auditory nerve, the inferior colliculus and its afferents) and best sensitivity
141 to modulation frequencies <100 Hz (Parthasarathy and Bartlett, 2012). The negative electrode was placed
142 under the right ear, along the mastoid, and the ground was placed in the nape of the neck. Impedances
143 were ensured to be always less than 1KΩ as tested using the low-impedance amplifier (RA4LI, TDT).

144 This two-channel setup allowed greater sensitivity to different ranges of modulation frequencies and
145 putative generators compared to recording from a single channel alone, as reported previously
146 (Parthasarathy and Bartlett, 2012). Signal presentation and acquisition were performed by BioSig

147 software (TDT). The stimulus was presented free field to the right of the animal, at a distance of 115 cm
148 from speaker to the right ear. Digitized waveforms were recorded with a multichannel recording and
149 stimulation system (RZ-5, TDT) and analyzed with BioSig or custom written programs in MATLAB
150 (Mathworks).

151 ***Surgical procedures for extracellular recordings***

152 Methods for surgery, sound stimulation and recording are similar to those described in (Herrmann et al.,
153 2015, Rabang et al., 2012). Surgeries and recordings were performed in a 9'×9' double walled acoustic
154 chamber (Industrial Acoustics Corporation). Animals were anesthetized using a mixture of ketamine
155 (VetaKet, 80 mg/kg) and dexmedetomidine (Dexdomitor, 0.2 mg/Kg) administered intra-muscularly via
156 injection. A constant physiological body temperature was maintained using a water-circulated heating
157 pad (Gaymar) set at 37°C with the pump placed outside the recording chamber to eliminate audio and
158 electrical interferences. The animals were maintained on oxygen through a manifold. The pulse rate and
159 oxygen saturation were monitored using a pulse-oximeter to ensure they were within normal ranges
160 during surgery. Supplementary doses of anesthesia (20mg/kg of ketamine, 0.05mg/kg of
161 dexmedetomidine) were administered intra-muscularly as required to maintain areflexia and a surgical
162 plane of anesthesia. An initial dose of dexamethasone and atropine was administered prior to incision to
163 reduce swelling and mucosal secretions. A subdermal injection of Lidocaine (0.5 ml) was administered
164 at the site prior to first incision. A central incision was made along the midline, and the calvaria exposed.
165 A stainless steel headpost was secured anterior to bregma using an adhesive and three screws drilled into
166 the skull to provide structural support for a head-cap, constructed of orthodontic resin (Dentsply). A
167 craniotomy was performed from 9–13 mm posterior to bregma, which extended posterior to the lambda
168 suture, and 3 mm wide extending from the midline. The dura mater was kept intact, and the site of
169 recording was estimated stereotaxically using a rat atlas (Paxinos and Watson, 2006) as well as using

internal vasculature landmarks and physiological measurements. At the completion of recordings, animals were euthanized with Beuthanasia (200 mg/kg IP). Once areflexive, they were perfused transcardially with 150-200 mL phosphate buffered saline with followed by 400–500 mL 4% paraformaldehyde. The brain was then removed and stored or processed further for Nissl or immunohistochemistry.

Electrophysiological recordings in extracellular space

Neural activity in inferior colliculus was recorded *in vivo* using a tungsten microelectrode (A-M Systems) encased in a glass capillary that was advanced using a hydraulic micro-drive (Narishige). We recorded 118 units in young rats and 121 units in aged rats. The inferior colliculus was identified based on short-latency driven responses to tone stimuli. The central nucleus of the inferior colliculus was identified using the ascending tonotopy moving in a dorsoventral direction as well as narrowly tuned responses to pure tones with frequencies ranging from 0.5 to 40 kHz. Recordings were obtained from both the dorsal cortex and central nucleus. Although we cannot exclude that we recorded from dorsal and lateral (or external) cortex, based on the recording depth, the presence of sustained responses to tones and amplitude-modulated stimuli, as well as clear frequency tuning in most cases, we estimate that most of our units were recorded from the central nucleus.

The sounds were presented to the animal at azimuth 0° and elevation 0°. Neural signals were acquired using the tungsten microelectrode connected to a headstage (RA4, TDT) and were amplified (RA4PA preamplifier, TDT). The digitized waveforms and spike times were recorded with a multichannel recording and stimulation system (RZ-5, TDT) at a sampling rate of 24.41 kHz (standard TDT sampling rate). The interface for acquisition and spike sorting were custom made using the OpenEx and RPvdsEx software (TDT). The units acquired were filtered between 500 Hz (occasionally 300 Hz) and 5000 Hz. The acquired spikes were stored in a data tank and analyzed using custom written software in Matlab.

Local field potentials were simultaneously recorded from the same electrode by sampling at 1525.88 Hz and bandpass filtering from 3 to 500 Hz.

Assessment of peripheral and brainstem function

Auditory brainstem responses (ABRs) were recorded using the scalp-recording setup described above. ABRs were recorded in response to brief broadband click stimuli of 0.1-ms duration that varied in sound levels from 5 to 95 dB SPL in 10 dB steps. The stimuli were presented in alternating polarity at 26.6 clicks per second. The acquisition window was 20 ms, and each ABR was an average of 1,500 repetitions. The ABR amplitudes of different waves were calculated as the amplitude of the peak of the wave from the baseline, in BioSig (TDT). ABRs between groups were compared at peak response level, which was determined as the lowest sound level that produced the maximum amplitude for each animal. This typically corresponded to 70–75 dB sound pressure level (SPL) for the young and 80–85 dB SPL for the aged rats.

Analysis of neural synchronization recorded at the scalp

For scalp recorded neural synchronization (i.e., EFRs), the speech-like stimulus (described above) was presented with a repetition rate of 3.1 Hz. The stimulus was presented at peak response level described above, which was determined following a fast-Fourier transform (FFT) of the time-domain response. Each response time course was obtained as an average of 200 stimulus repetitions in alternating polarity. Responses were filtered online between 30–3000 Hz with a 60 Hz notch filter.

In order to analyze the fidelity of the auditory system to synchronize with the temporal structure in the speech-like sound, we first used a broad-scale approach by calculating the correlation between the stimulus waveform and the response time course for lags ranging from 0 to 0.05 s. This cross-correlation approach was calculated twice, once for a low-frequency range (i.e., stimulus waveform and response time course were low-pass filtered at 300 Hz; Butterworth) and once for a high-frequency range (i.e.,

stimulus waveform and response time course were band-pass filtered from 300 to 3000 Hz; Butterworth). The former assessed neural synchronization to the vowel-like envelope periodicity, the latter assessed neural synchronization to the temporal fine structure in the stimulus. The highest correlation value (out of all lags) was used as a measure of synchronization strength. Separately for the two channels and the two filtered signals, Wilcoxon's rank sum test (Matlab: ranksum) was used to test whether correlation values differed between age groups.

We further investigated neural synchronization by calculating the amplitude spectrum (using a fast Fourier transform [FFT]; Hann window; zero-padding) of the averaged time-domain signal. Neural synchronization could not be quantified as inter-trial phase coherence (Lachaux et al., 1999) because the recordings were averaged across trials online. This analysis focused on neural synchronization to the envelope of the speech-like sound (~110 Hz) and we thus averaged the spectral amplitudes in the frequency window ranging from 105–115 Hz. Wilcoxon's rank sum test (Matlab: ranksum) was used to test whether neural synchronization to the envelope differed between age groups (separately for the caudal and rostral channel).

Analysis of local field potentials (LFPs)

Local field potentials previously band-pass filtered between 3-500Hz during acquisition were further notch filtered at 60 Hz and 120 Hz (elliptic filter; infinite-impulse response [IIR}; zero-phase lag) to suppress line noise, and low-pass filtered at 200 Hz (Butterworth; IIR; zero-phase lag).

For the time-domain analysis, single-trial time courses were averaged separately for each age group. Onset responses were analyzed by calculating the root-mean-square (RMS) amplitude of the averaged signal in the 0–0.08 s time window. Wilcoxon's rank sum test (Matlab: ranksum) was used to test differences in sound-onset responses between age groups.

238 Neural synchronization was analyzed by calculating a normalized vector strength spectrum (Wolff
239 et al., 2017, Herrmann et al., 2017). To this end, for each trial, a fast Fourier transform (FFT; Hann
240 window; zero-padding) was calculated using the data ranging from 0.08 s to 0.225 s post sound onset
241 (frequency range: 20–180 Hz; step size: 0.05 Hz; zero-padding) to exclude onset and offset transients.
242 An inter-trial phase coherence (ITPC) spectrum was calculated using the complex values from the FFT
243 (Lachaux et al., 1999). An ITPC permutation distribution was generated by flipping the sign of a random
244 subset of trials (Wolff et al., 2017), followed by ITPC calculation. This procedure was repeated 200 times
245 and resulted in a permutation distribution of ITPC values. The spectrum of normalized vector strength
246 was calculated by subtracting the mean ITPC of the permutation distribution from the empirically
247 observed ITPC and dividing the result by the standard deviation of the permutation distribution
248 (separately for each frequency). The normalized ITPC (vector strength) reflects a statistical measure –
249 that is, a z-score – with a meaningful zero that indicates non-synchronized activity.

250 In order to test for differences in neural synchronization at the envelope frequency between age
251 groups, the normalized vector strength was averaged across the 105–115 Hz frequencies. Wilcoxon's
252 rank sum test (Matlab: ranksum) was used to test whether neural synchronization differed between age
253 groups.

254 *Analysis of multi-unit activity (MUA)*

255 Multi-unit activity was extracted based on the recorded broad-band neural signal (Lakatos et al., 2013,
256 Lakatos et al., 2005). To this end, the signal was high-pass filtered at 300 Hz (Butterworth; IIR; zero-
257 phase lag), full-wave rectified by calculating absolute values, low-pass filtered at 200 Hz (Butterworth;
258 IIR; zero-phase lag), and down-sampled to the sampling frequency of the LFP (1525.88 Hz). Data
259 analysis followed closely the analysis of LFP data.

For the time-domain analysis, single-trial time courses were averaged separately for each age group. Onset responses were analyzed by calculating the mean amplitude of the averaged signal in the 0–0.08 s time window. Wilcoxon's rank sum test (Matlab: ranksum) was used to test differences in sound-onset responses between age groups.

Neural synchronization was analyzed by calculating a normalized vector strength spectrum using the same procedure as described for the LFP data.

Analysis of single-unit activity (SUA)

Overall, we recorded from 89 single units in young, and 123 single units in the aged animals. Single unit activity was isolated online during the recordings of the neural signals. Units that were substantially above noise threshold were sorted visually online, and then subsequently identified and isolated based on waveform similarity offline, using the OpenEx interface. Isolated single units had an SNR of at least 6 dB relative to the surrounding noise floor and stable waveform shapes. The acquired spikes were stored in data tank and analyzed using custom-written software in MATLAB.

Peri-stimulus time histograms were calculated by convolving an impulse vector generated from spike times with a Gaussian function with a standard deviation of 3 ms (Dayan and Abbott, 2001). Neural responses to the onset of the sound was investigated by calculating the mean firing rate for the 0–0.08 s time window. Wilcoxon's rank sum test (Matlab: ranksum) was used to test differences in sound-onset responses between age groups.

Investigation of neural synchronization was assessed using normalized vector strength based on spike times (Herrmann et al., 2017). To this end, spike times (within the 0.08–0.225 s time window) were transformed to phase angles ($\boldsymbol{p}$) using the following formula:

$$\boldsymbol{p} = 2\, f\, \boldsymbol{t}\, \pi + \pi$$

, where f is frequency and $\boldsymbol{t}$ a vector of spike times. Phase angles were wrapped to range from –π to π. The empirical vector strength v (similar to ITPC described above), that is, the resultant vector length, was calculated as follows (Lachaux *et al.*, 1999):

$$v = \frac{1}{n}\left|\sum_{j=1}^{n} e^{ip_j}\right|$$

, where v is the vector strength, i the imaginary unit, $\boldsymbol{p}$ the vector of phase angles, and n the number of spikes (with j being the index). Vector strength can be biased by the number of spikes, with smaller v values for a higher number of spikes. In order to avoid biases estimates, a distribution of random vector strength values was calculated. That is, n (number of spikes) random phase values between –π and π were generated and the vector strength (i.e., the resultant vector length) was calculated. Randomly drawing phase values and calculation of the vector strength was repeated 1000 times, which resulted in a distribution of random vector strengths given the number of spikes. The normalized vector strength was then calculated by subtracting the mean of the random vector strength distribution from the empirical vector strength and dividing the result by the standard deviation of the random vector strength distribution. The normalized vector strength was calculated for frequencies (f) ranging from 20 Hz to 180 Hz with a frequency resolution of 0.1 Hz, resulting in a vector strength spectrum. In order to test for differences in neural synchronization at the envelope frequency between age groups, the normalized vector strength was averaged across the 105–115 Hz frequencies. Wilcoxon's rank sum test was used to test whether neural synchronization differed between age groups.

Effect size measure

Throughout the manuscript, effect sizes are provided as r_e ($r_{equivalent}$; Rosenthal and Rubin, 2003). r_e is equivalent to a Pearson product-moment correlation for two continuous variables, to a point-biserial

correlation for one continuous and one dichotomous variable, and to the square root of partial η^2 for an analysis of variance.

RESULTS

ABR amplitudes are reduced in aged animals

ABRs were recorded simultaneously from two electrode montages – one that emphasizes more caudal generators (putatively including the auditory nerve and the cochlear nucleus), and another that emphasizes more rostral generators (putatively including the inferior colliculus), as evidenced by the differences in ABR waveform morphology, modulation rate sensitivity, and the effects of anesthesia (Parthasarathy and Bartlett, 2012, Parthasarathy et al., 2014).

ABR wave 1 amplitudes were significantly decreased for aged compared to young rats (Figure 2A, rostral channel: $p = 1.96^{e-4}$, $r_e = 0.701$, df = 21; caudal channel: $p = 7.20^{e-5}$, $r_e = 0.732$, df = 21). The wave 1 of the ABR originates in the auditory nerve, and its amplitude at suprathreshold sound levels is a physiological indicator for the degree of cochlear synaptopathy due to aging or noise exposure (Sergeyenko et al., 2013, Stamper and Johnson, 2015). This age-related decrease in ABR amplitudes was also observed for all subsequent waves (wave 3: $p = 5.55^{e-5}$, $r_e = 0.739$, df = 21; wave 4: $p = 9.92^{e-4}$, $r_e = 0.641$, df = 21; wave 5: $p = 7.17^{e-5}$, $r_e = 0.732$, df = 21; Figure 2A) with generators in other brainstem and midbrain nuclei. Hence, there was an overall reduction in transient responses in the auditory nerve fibers, auditory brainstem and midbrain with age.

Scalp-recorded neural synchronization shows strong spectral peaks and stimulus correlation with age despite weak ABR amplitudes

The ability of the auditory system to represent the various temporal regularities of speech were assessed using a measure of neural synchronization (i.e., EFR) evoked to the speech-like sound. The sensitivity

of neural activity to the sound's temporal structure was assessed in two ways: Cross-correlation and spectral amplitude (derived from a fast Fourier transform). The overall temporal sensitivity was calculated by cross-correlating the time course of the scalp-recorded neural response with the stimulus time course. In the caudal channel, cross-correlation values were reduced for aged compared to young rats ($p = 1.54^{e-4}$, $r_e = 0.709$, df = 21) for the 300–3000-Hz frequency range that contains information about the sound's temporal fine structure. There was no difference in correlation values between young and aged animals for the <300-Hz frequency range (envelope) ($p = 0.479$, $r_e = 0.155$, df = 21; Figure 2B, left). In the rostral channel with putative generators in the midbrain and its afferents, there was no age difference for the 300–3000-Hz frequency range ($p = 0.069$, $r_e = 0.385$, df = 21). However, aging was associated with an increase in correlation values for the <300 Hz range (envelope) ($p = 0.034$, $r_e = 0.444$, df = 21; Figure 2B, right).

Spectral amplitudes derived via a fast Fourier transform were averaged in the 105–115 Hz frequency band to assess neural synchronization to the temporal envelope (i.e., fundamental frequency; F0) of the speech-like sound. For the caudal channel, neural synchronization at the envelope frequency was larger for young compared to aged rats ($p = 1.96^{e-4}$, $r_e = 0.701$, df = 21; Figure 2C, left). Although there was a similar trend in the rostral channel, this was not statistically significant ($p = 0.069$, $r_e = 0.385$, df = 21; Figure 2C, right).

Taken together, our neural synchronization measures show that for caudal generators (auditory nerve, cochlear nucleus) synchronization was either similar or increased for younger compared to aged rats, whereas for rostral generators (lateral lemniscus, inferior colliculus) synchronization was either similar or increased for aged compared to younger rats. These data may suggest an age-related relative increase in synchronization strength along the ascending auditory pathway. Extracellular recordings from inferior colliculus neurons were obtained to further explore the age-related gain increases in the auditory system to the complex, speech-like sound.

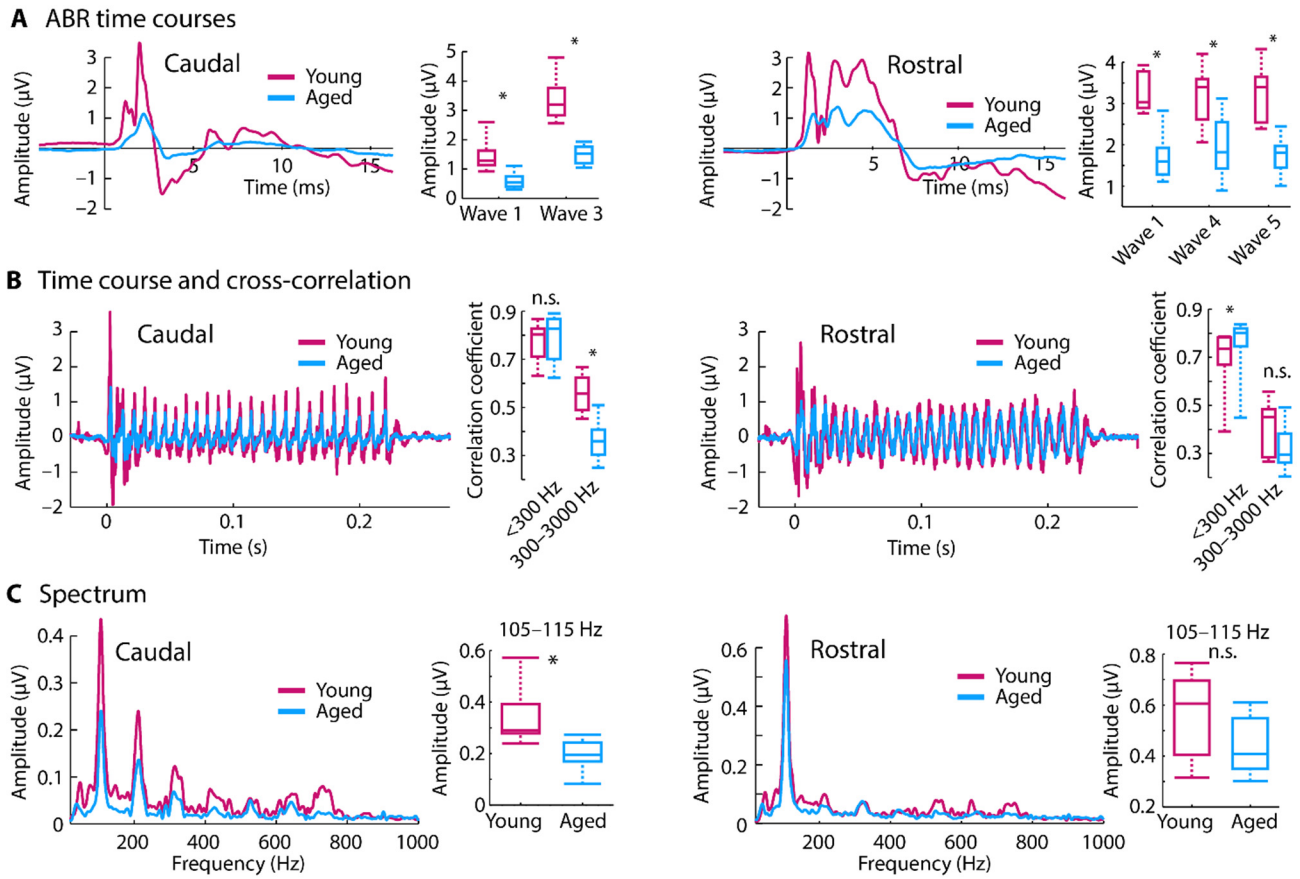

Figure 2: Scalp-recorded potentials simultaneously recorded in two channels emphasizing rostral versus caudal generators. A: Averaged click-evoked auditory brainstem responses (ABRs) and amplitudes for different ABR waves. **B:** Time courses of envelope following responses (EFRs) in response to the speech-like /ba/ sound. Boxplots show coefficients from the cross-correlation for different frequency bands. **C:** Amplitude spectra derived from fast Fourier transforms. Boxplots show neural synchronization strength to the sound's F0 envelope (105–115 Hz). *p < 0.05, n.s. – not significant

LFP onset response and neural synchronization to the envelope are reduced in aged animals

Although changes in the neural representation of the speech-like sound were observed in the scalp-recorded synchronization measures, these EFRs reflect the superposition of activity from multiple generators. In order to localize age-related changes to the inferior colliculus and its afferents, we used LFPs as a proxy for the synaptic input to the inferior colliculus neurons. LFP time courses are displayed

in Figure 3A. Neural responses to the sound onset (RMS amplitude 0–0.08 s) was larger for young compared to aged animals ($p = 4.47^{e-9}$, $r_e = 0.368$, df = 237; Figure 3A right), suggesting that the strength of the synaptic inputs to the inferior colliculus neurons decrease with age.

In order to investigate whether this decrease in synaptic input is accompanied by a decrease in LFP synchronization, the normalized vector strength at the F0 frequency (105–115 Hz) was measured in the sustained response of the LFP (0.08–0.225 s; Figure 3B). Neural synchronization was larger for young compared to aged rats ($p = 2.66^{e-4}$, $r_e = 0.234$, df = 237). These results indicate that the synaptic inputs to the inferior colliculus neurons in response to a speech-like sound decrease in amplitude and synchrony with age.

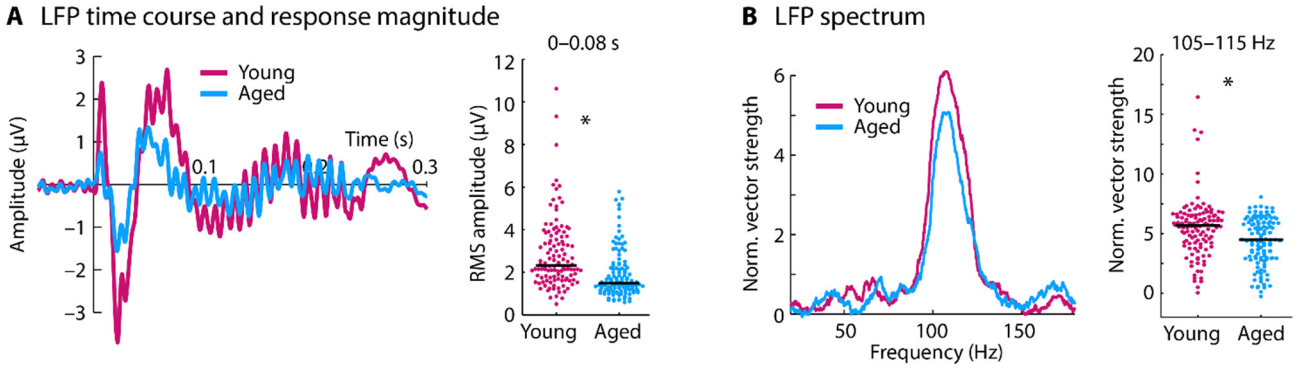

Figure 3: Time course and spectrum for local field potentials. A: Time course for each age group (left) and the root mean square (RMS) amplitude for the 0–0.08 s time window (right). **B:** Spectrum of normalized vector strength (left) and the mean vector strength for the 105–115 Hz frequency window (right). In panel A and B, each dot reflects the normalized vector strength of an individual unit. The black horizontal line reflects the median across units. *p < 0.05

Synchronization of multi-unit activity with the speech envelope are increased with age

In order to investigate the consequences of the age-related decrease in synaptic inputs (indicated by the LFPs) on the neural output of inferior colliculus neurons, multi-unit spiking activity was used as a proxy for neural population or network responses in the inferior colliculus. Time courses for the multi-unit activity (MUA) are shown in Figure 4. Spontaneous activity, quantified as the mean response in the time

window preceding sound onset (–0.05–0 s), was larger in aged compared to young rats ($p = 2.91^{e-10}$, r_e = 0.393, df = 237; box plots in Figure 4A, left). Unlike the onset amplitudes of the LFPs (for which responses were reduced for aged animals), there was no difference in MUA neuronal responses to the sound onset (amplitude in the 0–0.08 s time window) between age groups (p = 0.894, re = 0.009, df = 237; Figure 4A, middle and right).

Synchronization of MUA with the envelope of the sound was quantified using normalized vector strength (Figure 4B). At the stimulation frequency (mean across the 105–115 Hz frequency window), neural synchronization was larger for aged compared to young rats ($p = 4.79^{e-9}$, r_e = 0.367, df = 237). Taken together, the LFP and MUA results suggest a relative increase in neural response and an increase in synchronization from a neuron's input to the neural population spiking output for aged compared to young animals.

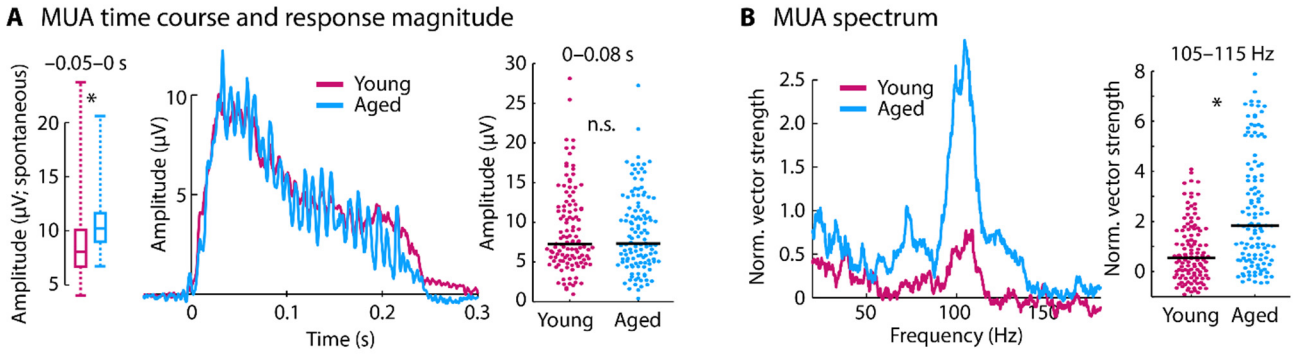

Figure 4: Time course and spectrum for multi-unit activity. A: Left: The box plots show the amplitude of the pre-stimulus onset time window (–0.05–0 s; i.e., spontaneous activity). Pre-stimulus onset activity was larger in aged compared to young animals ($p < 0.05$). Middle: Time course for each age group (data are baseline corrected, i.e., the mean response in the –0.05–0 s time window was subtracted from the amplitude at each time point). Right: Mean amplitude for the 0–0.08 s time window. **B:** Spectrum of normalized vector strength (left) and the mean vector strength for the 105–115 Hz frequency window (right). In panel A and B, each dot reflects the normalized vector strength of an individual unit. The black horizontal line is the median across units. *$p < 0.05$

Synchronization of single-unit activity with the speech envelope are similar between young and aged animals

Neuronal activity from well isolated neurons (single-unit activity) was analyzed in order to investigate whether individual neurons in the aged inferior colliculus also show a relative enhancement of onset-evoked activity and synchronization to the envelope.

Peri-stimulus time histograms for single-unit activity (SUA) are shown in Figure 5. Spontaneous firing rates (i.e., in the –0.05–0 s time window) did not differ between age groups ($p = 0.831$, $r_e = 0.015$, $df = 210$). Firing rates to the sound onset (0–0.08 s) were larger for young compared to aged animals ($p = 1.02^{e-4}$, $r_e = 0.268$, $df = 210$; Figure 5A). Neural synchronization to the envelope (F0) of the sound measured using normalized vector strength showed no effect of age (mean across the 105–115 Hz frequency window; $p = 0.703$, $r_e = 0.026$, $df = 210$; Figure 5B). Given the reduced LFP synchronization, these results suggest an age-related increase in neural synchronization in single unit activity (a neuron's output) relative to the LFP (synaptic input), albeit to a lesser degree than for multi-unit activity.

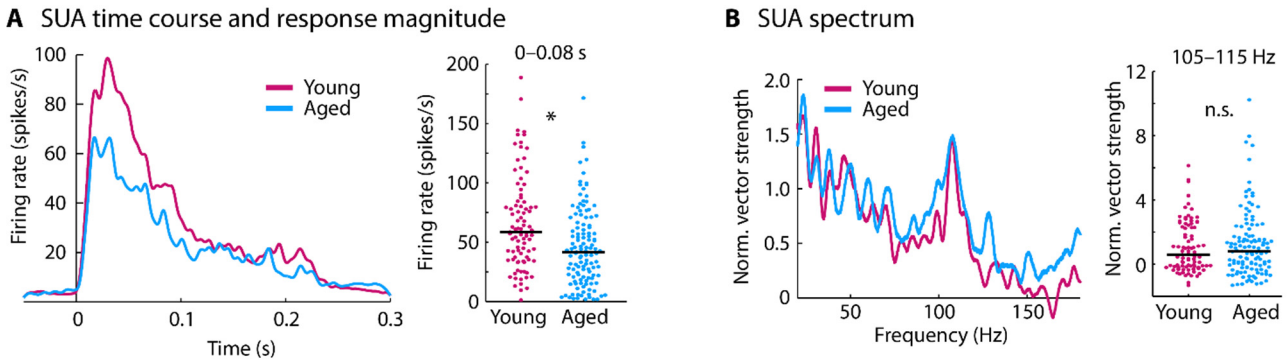

Figure 5: Time course and spectrum for single-unit activity. A: Peri-stimulus time histogram for each age group (left) and mean firing rate for the 0–0.08 s time window (right). **B:** Spectrum of normalized vector strength (left) and the mean vector strength for the 105–115 Hz frequency window (right). In panel A and B, each dot reflects the normalized vector strength of an individual unit. The black horizontal line is the median across units. *$p < 0.05$

Aging affects the relative change from LFP to spiking activity

In order to quantify the effects of aging on the relative changes from the local field potential to spiking activity, we calculated the normalized difference between the LFP and SUA, and between the LFP and MUA. In detail, the LFP, SUA, and MUA were separately z-transformed by subtracting the mean and dividing by the standard deviation (including data points from young and aged rats). The z-transformation was separately calculated for onset responses (i.e., RMS or mean for the 0–0.08 s time window, for LFP and spiking activity, respectively) and neural synchronization (i.e., the mean normalized vector strength for the 105–115 Hz frequency window). For the LFP-to-SUA change, we subtracted the z-transformed LFP measure from the z-transformed SUA measure. The LFP-to-MUA change was calculating similarly by using the MUA instead of the SUA.

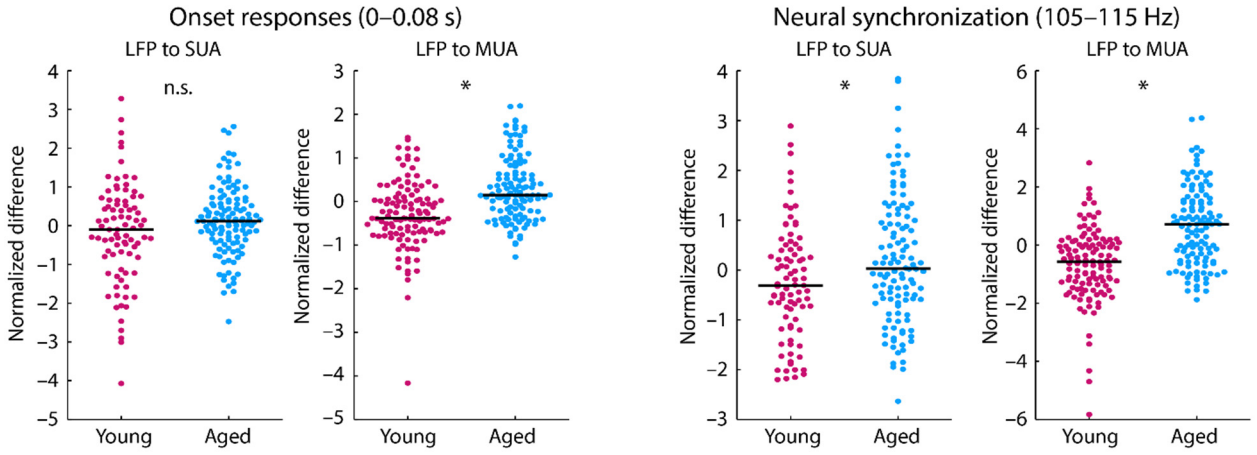

Figure 6: Normalized difference between local field potential and spiking activity (SUA and MUA). Left: Normalized difference for onset responses (time window from 0 to 0.08 s). **Right:** Normalized difference for neural synchronization in the 0.08-0.225s time window (frequency window from 105 to 115 Hz). Each dot reflects an individual unit. The black horizontal line is the median across units *p < 0.05; n.s. – not significant.

Wilcoxon's rank sum test was used to test for differences between age groups (Figure 6). For onset responses, there was no difference between age groups for the relative change from LFP to SUA ($p = 0.103$, $r_e = 0.115$, df = 202), but a significantly larger change from LFP to MUA in aged compared to young rats ($p = 1.47^{e-8}$, $r_e = 0.356$, df = 237). For neural synchronization, the change from LFP to SUA

($p = 0.018$, $r_e = 0.167$, $df = 199$) as well as the change from LFP to MUA ($p = 7.10^{e-12}$, $r_e = 0.425$, $df = 237$) was increased for aged compared to young rats.

Neural responses to a natural stimulus also show enhanced envelope sensitivity

In order to examine whether the observed effects using the noise carrier also translate to real speech, we additionally recorded neural activity in response to the original /ba/ speech sound for a subset of units. Neurons responsive to this stimulus were found in lesser numbers due to the differences in the frequency sensitivity of the rat's hearing range. Local field potentials and multi-unit activity was recorded for 52 units in young animals and 20 units in aged animals. Single-unit activity was available for 33 units in young animals and 20 units in aged animals.

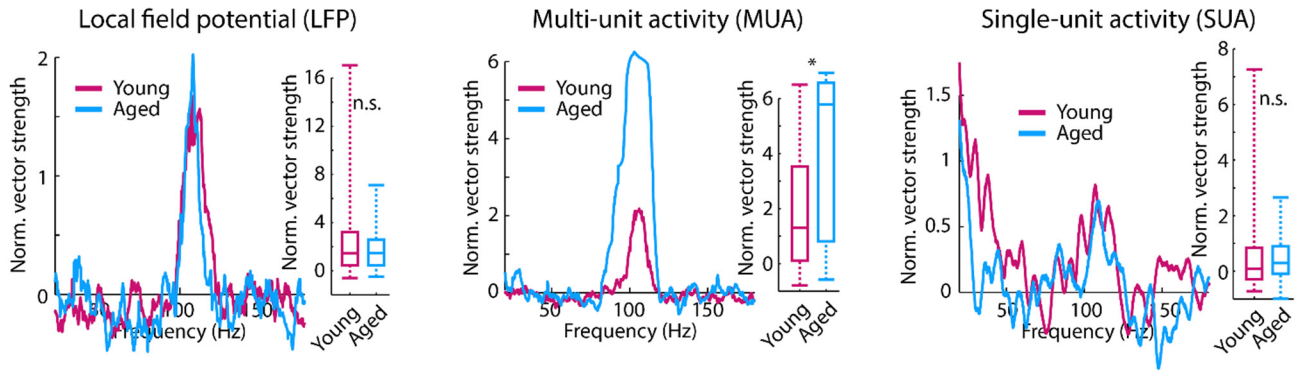

Figure 7: Spectrum of normalized vector strength for LFPs, MUA, and SUA in response to a speech sound. Box plots show the mean normalized vector strength for the 105–115 Hz frequency window. *$p < 0.05$, n.s. – not significant

The spectrum of normalized vector strength was calculated for LFPs, MUA, and SUA. The results are displayed in Figure 7 and approximately mirror the results reported for the noise carrier. Effects of aging on neural synchronization to the stimulus envelope were assessed by comparing the mean normalized vector strength in the 105–115 Hz frequency window between age groups. For LFPs, there was no difference in neural synchronization between age groups ($p = 0.730$, $r_e = 0.042$, $df = 70$). An age-related increase in synchronization with the sound's envelope was observed for the MUA ($p = 9.78^{e-3}$, r_e

423 = 0.303, df = 70). For SUA, there was no effect of age for neural synchronization to the envelope of the
424 stimulus ($p = 0.345$, $r_e = 0.132$, df =51).

425 **DISCUSSION**

426 In the current study, we used a systems level (scalp recordings) and a micro-circuit level (LFPs and unit
427 activity) approach to investigate the age-related changes in neural sensitivity to temporal regularity in a
428 speech-like sound. Scalp-recorded potentials indicate that aging leads to a relative increase in neural
429 synchronization to the periodicity envelope along the ascending auditory pathway. The underlying
430 cellular changes in the midbrain were examined by recording neural activity from neurons in the inferior
431 colliculus in response to the speech-like sound. We used the local field potential as a proxy for a neuron's
432 or neural population's synaptic inputs, and multi-unit and single-unit activity as a measure of spiking
433 output. LFP amplitudes to the sound onset and LFP neural synchronization to the temporal regularity of
434 the envelope were smaller in aged compared to young rats. In contrast, multi-unit activity and, to a lesser
435 degree, single unit activity showed an aged-related relative increase in synchronization to the periodicity
436 envelope. Our results suggest that aging is associated with altered sensitivity to sounds and a sound's
437 temporal regularities, and that these effects may be due to altered gain in neural network activity in the
438 aged auditory midbrain.

439 ***Scalp-evoked potentials point to a decrease in brainstem responses and an increase in***
440 ***inferior colliculus responses***

441 Auditory brainstem responses (ABRs) and neural synchronization (i.e., EFRs) have been used to study
442 age-related changes in neural activity to speech and other complex sounds in humans (Stamper and
443 Johnson, 2015, Clinard and Tremblay, 2013, Anderson et al., 2012). The ability to obtain these responses
444 non-invasively makes them an ideal bridge between human studies and studies in animal models, for

445 which the underlying pathophysiology can additionally be studied at the micro-circuit level using more
446 invasive techniques (Zhong et al., 2014, Shaheen et al., 2015).

447 Consistent with previous studies (Fernandez et al., 2015, Sergeyenko et al., 2013, Parthasarathy
448 et al., 2014), we observed an age-related decrease in the wave 1 amplitude of the ABR to clicks at
449 suprathreshold sound levels (Figure 2A). The wave 1 of the ABR at suprathreshold sound levels may be
450 considered as a physiological indicator for the degree of cochlear synaptopathy, that is, the loss of
451 synapses between the inner hair cells and the auditory nerve fibers (Kujawa and Liberman, 2009, Konrad-
452 Martin et al., 2012). This cochlear synaptopathy has been observed in aging and noise-exposed animals,
453 including mice (Sergeyenko et. al., 2013, Fernandez et. al., 2015), rats (Mohrle et. al., 2016), gerbils
454 (Gleich et. al., 2016), guinea pigs (Furman et. al., 2013, Schmeidt et. al., 1996), and macaques (Valero
455 et. al., 2017), in addition to evidence from post-mortem human temporal bones (Viana et. al., 2015). The
456 reduction of wave 1 in aged compared to young rats thus suggests the presence of cochlear synaptopathy
457 in the aged population used in the current study.

458 The sensitivity of the scalp-recorded EFRs to regular temporal structure in a speech-like sound was
459 investigated using measures of neural synchronization. We observed reduced synchronization to the
460 envelope and fine structure information for activity likely originating in the auditory nerve and cochlear
461 nucleus (Figure 2, left). Signals likely originating from rostral generators, including the inferior
462 colliculus, showed an age-related increase in neural synchronization to the envelope of the speech-like
463 sound (Figure 2B, C). These results suggest an age-related transformation in the neural representation of
464 envelope cues in speech along the ascending auditory pathway, which we investigated further using more
465 invasive extracellular electrophysiological methods.

466 ***Aging increases network level activity of inferior colliculus neurons relative to their***
467 ***synaptic inputs***

468 In order to study the contributions of the auditory midbrain to the changes seen in the scalp-recorded
469 responses, we simultaneously recorded LFPs and unit responses from the same site in response to sound.
470 LFPs are thought to be largely the aggregate pre-synaptic activity at the dendrites and the soma, and
471 hence a proxy for the inputs to the neuron or neuronal region (Buzsaki et al., 2012, Gourevitch and
472 Edeline, 2011, Logothetis and Wandell, 2004, Logothetis et al., 2001). By comparing these LFPs to the
473 spiking output, the transformation of these sound representations in the inferior colliculus can be
474 investigated (Herrmann et al., 2017).

475 In the current study, LFPs to the sound onset and neural synchronization to the sound's envelope
476 were decreased for aged compared to young rats (Figure 3), suggesting that inputs to the inferior
477 colliculus neurons are degraded. In contrast, multi-unit spiking activity in the inferior colliculus –
478 reflecting population or network output – revealed no age difference in the onset response and age-related
479 increase in synchronization to the sound's envelope (Figure 4). This relative enhancement seen at the
480 population level (MUA) was also present, albeit to a lesser degree, at the level of the single neurons
481 (SUA, Figures 5 and 6). These results suggest that the inferior colliculus neurons selectively increase
482 their neuronal activity to the envelope of a speech-like sound in aged animals, despite the reduced
483 synaptic inputs to these neurons.

484 Previous work suggested that midbrain neurons responding to simple stimuli like tones and noise
485 bursts show remarkably subtle changes with age (Willott et al., 1988a, Willott et al., 1988b). This is
486 despite the extensive degradation of the peripheral auditory system, such as the loss of outer hair cells
487 (Chen et al., 2009, Spongr et al., 1997), changes in endocochlear potential (Ohlemiller et al., 2006), and
488 the loss of cochlear synapses (Sergeyenko et al., 2013) and spiral ganglion neurons in the auditory nerve
489 (Bao and Ohlemiller, 2010). Even when studies using single-unit recordings do find age-related changes

in temporal processing (Palombi et al., 2001, Walton et al., 2002), it is unclear whether these changes are inherited from previous stages of auditory processing, or generated in the nucleus being studied. Our approach in this study shows that the enhancements seen in the spiking output of the inferior colliculus neurons, in particular at the population and network level, may explain some of this dichotomy in peripheral versus central responses with age.

Potential mechanisms underlying age-related changes in sensitivity to temporal regularity in sounds

Acute insults (e.g., ototoxic drugs or mechanical deafening) to the auditory system damages the auditory periphery and triggers homeostatic changes in the auditory pathway (Kotak et al., 2005, Chambers et al., 2016). The most drastic change reported is a loss of inhibitory circuits and function (Resnik and Polley, 2017, Caspary et al., 2013, Richardson et al., 2013, Ling et al., 2005), which, in turn, increases neuronal activity in the central auditory structures (Chambers et al., 2016). The current data in combination with recent evidence suggests that central auditory systems undergo similar gain increases when the peripheral insult is gradual as is the case for aging (Lai et al., 2017, Parthasarathy et al., 2014, Presacco et al., 2016).

The increase in neuronal activity due to a loss of inhibition is typically accompanied by a reduction in the precision of neural coding. Inferior colliculus neurons change their tuning curves to become less selective with age (Leong et al., 2011, Rabang et al., 2012). In addition, sensitivity to temporal regularities in simple stimuli increases for slow amplitude modulations but decreases for fast amplitude modulations in aged animals (Walton et al., 2002, Herrmann et al., 2017). In the current study, inferior colliculus neurons in aged animals showed an increase in the spontaneous firing rate (Figure 4A), which suggests inhibition was reduced in the aged midbrain. Furthermore, despite reduced synaptic inputs to inferior colliculus neurons (as indexed by our LFP recordings), neuronal firing of populations of inferior colliculus neurons was overly synchronized with the envelope of a speech-like sound in aged compared

513 to young animals (Figures 3 and 4). Our data thus suggest that temporal response precision is altered in
514 the aged midbrain due to hypersensitivity in networks of neurons.

515 Increased gain in the auditory system may lead to better detection of weak signals in neural circuits,
516 and may, in turn, support hearing in quiet environments (Chambers et. al., 2016). For example, hearing
517 loss has been shown to increase sensitivity to suprathreshold amplitude modulation in sounds (Moore et
518 al. 1996). However, neural gain enhancements may come at the cost of poor discrimination between
519 stimuli (Guo et al., 2017). For example, discrimination between fundamental frequency in speech is
520 reduced for older adults with clinically normal audiograms (Vongpoisal and Pichora-Fuller, 2007), and
521 a gain increase in cortex has been linked to poor speech perception in the presence of competing sound
522 (Millman et al., 2017). Hence, an aberrant neural gain increase in aging may not be beneficial for listening
523 to sounds that are typical of everyday life, such as speech, when perception requires the segregation of
524 different concurrent sounds.

525 **CONCLUSIONS**

526 We investigated how aging affects neural sensitivity to temporal regularity in a speech-like sound.
527 Systems level recordings (i.e., at the scalp) were combined with microcircuit recordings (i.e., LFPs and
528 unit activity recorded extracellularly) in young and aged rats. We show that aging is associated with
529 increased neural activity along the ascending auditory pathway, which alters the sensitivity of midbrain
530 (i.e., inferior colliculus) neurons to temporally regular structure in sounds. Specifically, synchronization
531 to the periodicity envelope in speech (at the fundamental frequency) was enhanced for spiking activity
532 of populations of inferior colliculus neurons in aged rats, despite the neuron's reduced synaptic input.
533 The data suggest that temporal response precision is altered in the aged midbrain due to hypersensitivity
534 in networks of neurons.

ACKNOWLEDGEMENTS

This study was supported by NIDCD DC-011580 to ELB.

REFERENCES

Allen, P. D. and Eddins, D. A. (2010) Presbycusis phenotypes form a heterogeneous continuum when ordered by degree and configuration of hearing loss. Hear Res 264(1-2):10-20.

Anderson, S., Parbery-Clark, A., White-Schwoch, T. and Kraus, N. (2012) Aging Affects Neural Precision of Speech Encoding. J Neurosci 32(41):14156-64.

Anderson, S., Parbery-Clark, A., Yi, H.-G. and Kraus, N. (2011) A Neural Basis of Speech-in-Noise Perception in Older Adults. Ear Hear 32(6): 750-757.

Bao, J. X. and Ohlemiller, K. K. (2010) Age-related loss of spiral ganglion neurons. Hear Res 264(1-2): 93-97.

Bregman, A. S. (1990) Auditory Scene Analysis; The Perceptual Organization of Sound. Cambridge, MA: MIT Press.

Bullock, T. H. (1997) 'Signals and signs in the nervous system: The dynamic anatomy of electrical activity is probably information-rich', Proceedings of the National Academy of Sciences of the United States of America, 94(1), pp. 1-6.

Buzsaki, G., Anastassiou, C. A. and Koch, C. (2012) The origin of extracellular fields and currents - EEG, ECoG, LFP and spikes. Nat Rev Neurosci 13(6): 407-420.

Caspary, D. M., Hughes, L. F. and Ling, L. L. (2013) Age-related GABA(A) receptor changes in rat auditory cortex. Neurobiol Aging. 34(5): 1486-1496.

Caspary, D. M., Ling, L., Turner, J. G. and Hughes, L. F. (2008) Inhibitory neurotransmission, plasticity and aging in the mammalian central auditory system. J Exp Biol. 211(11): 1781-1791.

Chambers, A. R., Resnik, J., Yuan, Y. S., Whitton, J. P., Edge, A. S., Liberman, M. C. and Polley, D. B. (2016) Central Gain Restores Auditory Processing following Near-Complete Cochlear Denervation. Neuron 89(4): 867-879.

Chen, G. D., Li, M. N., Tanaka, C., Bielefeld, E. C., Hu, B. H., Kermany, M. H., Salvi, R. and Henderson, D. (2009) Aging outer hair cells (OHCs) in the Fischer 344 rat cochlea: Function and morphology. Hear Res 248(1-2): 39-47.

Clinard, C. G. and Tremblay, K. L. (2013) Aging Degrades the Neural Encoding of Simple and Complex Sounds in the Human Brainstem. J Am Acad Audiol 24(7): 590-599.

Dayan, P. and Abbott, L. F. (2001) Theoretical neuroscience: computational and mathematical modeling of neural systems. Cambridge, MA, USA: MIT Press.

Drummond, G. B. (2009) Reporting ethical matters in The Journal of Physiology: standards and advice. J Physiol. 587: 713-719.

Dubno, J. R., Eckert, M. A., Lee, F. S., Matthews, L. J. and Schmiedt, R. A. (2013) Classifying Human Audiometric Phenotypes of Age-Related Hearing Loss from Animal Models. J Assoc Res Otolaryngol. 14(5): 687-701.

Fernandez, K. A., Jeffers, P. W. C., Lall, K., Liberman, M. C. and Kujawa, S. G. (2015) Aging after Noise Exposure: Acceleration of Cochlear Synaptopathy in "Recovered" Ears. J Neurosci 35(19): 7509-7520.

Frisina, D. R. and Frisina, R. D. (1997) Speech recognition in noise and presbycusis: Relations to possible neural mechanisms. Hear Res 106(1-2): 95-104.

Fullgrabe, C., Moore, B. C. J. and Stone, M. A. (2015) Age-group differences in speech identification despite matched audiometrically normal hearing: contributions from auditory temporal processing and cognition. Front Aging Neurosci 6:347.

Furman, A. C., Kujawa, S. G. and Liberman, M. C. (2013) Noise-induced cochlear neuropathy is selective for fibers with low spontaneous rates, Journal of Neurophysiology, 110(3), pp. 577-586.

Gleich, O., Semmler, P. and Strutz, J. (2016) Behavioral auditory thresholds and loss of ribbon synapses at inner hair cells in aged gerbils, Experimental Gerontology, 84, pp. 61-70.

Gordon-Salant, S. and Fitzgibbons, P. J. (2001) Sources of age-related recognition difficulty for time-compressed speech. J Speech Lang Hear Res. 44(4): 709-719.

Gourevitch, B. and Edeline, J. M. (2011) Age-related changes in the guinea pig auditory cortex: relationship with brainstem changes and comparison with tone-induced hearing loss. Eur J Neurosci. 34(12): 1953-1965.

Guo, W., Clause, A. R., Barth-Maron, A. and Polley, D. B. (2017) A Corticothalamic Circuit for Dynamic Switching between Feature Detection and Discrimination. Neuron, 95(1): 180-194.

Herrmann, B., Parthasarathy, A. and Bartlett, E. L. (2017) Ageing affects dual encoding of periodicity and envelope shape in rat inferior colliculus neurons. Eur J Neurosci 45(2): 299-311.

Herrmann, B., Parthasarathy, A., Han, E. X., Obleser, J. and Bartlett, E. L. (2015) Sensitivity of rat inferior colliculus neurons to frequency distributions. J Neurophysiol. 114: 2941-2954.

Hughes, L. F., Turner, J. G., Parrish, J. L. and Caspary, D. M. (2010) Processing of broadband stimuli across A1 layers in young and aged rats. Hear Res. 264(1-2): 79-85.

Konrad-Martin, D., Dille, M. F., McMillan, G., Griest, S., McDermott, D., Fausti, S. A. and Austin, D. F. (2012) Age-Related Changes in the Auditory Brainstem Response. J Am Acad Audiol. 23(1): 18-35.

Kotak, V. C., Fujisawa, S., Lee, F. A., Karthikeyan, O., Aoki, C. and Sanes, D. H. (2005) Hearing loss raises excitability in the auditory cortex. J Neurosci. 25(15): 3908-3918.

Kujawa, S. G. and Liberman, M. C. (2009) Adding Insult to Injury: Cochlear Nerve Degeneration after "Temporary" Noise-Induced Hearing Loss J Neurosci. 29(45): 14077-14085.

Lachaux, J.-P., Rodriguez, E., Martinerie, J. and Varela, F. J. (1999) Measuring Phase Synchrony in Brain Signals. Hum Brain Mapp 8: 194-208.

Lai, J., Sommer, A. L. and Bartlett, E. L. (2017) Age-related changes in envelope-following responses at equalized peripheral or central activation. Neurobiol Aging. 58: 191-200.

Lakatos, P., Musacchia, G., O'Connel, M. N., Falchier, A. Y., Javitt, D. C. and Schroeder, C. E. (2013) The Spectrotemporal Filter Mechanism of Auditory Selective Attention. Neuron, 77(4): 750-761.

Lakatos, P., Shah, A. S., Knuth, K. H., Ulbert, I., Karmos, G. and Schroeder, C. E. (2005) An oscillatory hierarchy controlling neuronal excitability and stimulus processing in the auditory cortex. J Neurophysiol 94(3): 1904-1911.

Leong, U. C., Barsz, K., Allen, P. D. and Walton, J. P. (2011) Neural correlates of age-related declines in frequency selectivity in the auditory midbrain. Neurobiol Aging, 32(1): 168-178.

Ling, L. L., Hughes, L. F. and Caspary, D. M. (2005) Age-related loss of the GABA synthetic enzyme glutamic acid decarboxylase in rat primary auditory cortex. Neuroscience. 132(4): 1103-1113.

Logothetis, N. K., Pauls, J., Augath, M., Trinath, T. and Oeltermann, A. (2001) Neurophysiological investigation of the basis of the fMRI signal. Nature, 412(6843): 150-157.

Logothetis, N. K. and Wandell, B. A. (2004) Interpreting the BOLD signal. Annu Rev Physiol 66: 735-769.

Millman, R. E., Mattys, S. L., Gouws, A. D. and Prendergast, G. (2017) 'Magnified Neural Envelope Coding Predicts Deficits in Speech Perception in Noise', Journal of Neuroscience, 37(32), pp. 7727-7736.

Mohrle, D., Ni, K., Varakina, K., Bing, D., Lee, S. C., Zimmermann, U., Knipper, M. and Ruttiger, L. (2016) Loss of auditory sensitivity from inner hair cell synaptopathy can be centrally compensated in the young but not old brain. Neurobiol Aging. 44: 173-184.

Moore, B. C. J., Wojtczak, M. and Vickers, D. A. (1996) 'Effect of loudness recruitment oil the perception of amplitude modulation', Journal of the Acoustical Society of America, 100(1), pp. 481-489.

632 Ohlemiller, K. K., Lett, J. M. and Gagnon, P. M. (2006) Cellular correlates of age-related endocochlear
633 potential reduction in a mouse model. Hear Res. 220(1-2): 10-26.
634 Palombi, P. S., Backoff, P. M. and Caspary, D. M. (2001) Responses of young and aged rat inferior
635 colliculus neurons to sinusoidally amplitude modulated stimuli. Hear Res 153(1-2): 174-180.
636 Parthasarathy, A. and Bartlett, E. (2012) Two-channel recording of auditory-evoked potentials to detect
637 age-related deficits in temporal processing. Hear Res 289(1-2): 52:62.
638 Parthasarathy, A., Datta, J., Torres, J. A. L., Hopkins, C. and Bartlett, E. L. (2014) Age-Related Changes
639 in the Relationship Between Auditory Brainstem Responses and Envelope-Following Responses. J
640 Assoc Res Otolaryngol. 15(4): 649-661.
641 Parthasarathy, A., Lai, J. and Bartlett, E. L. (2016) Age-Related Changes in Processing Simultaneous
642 Amplitude Modulated Sounds Assessed Using Envelope Following Responses. J Assoc Res
643 Otolaryngol 17(2): 119-132.
644 Paxinos, G. and Watson, C. (2006) The Rat Brain in Stereotaxic Coordinates. Academic Press.
645 Pichora-Fuller, M. K. and Souza, P. E. Effects of aging on auditory processing of speech. Workshop on
646 Candidature for and Delivery of Audiological Services - Special Needs of Older People, Eriksholm,
647 Denmark, Nov: B C Decker Inc, S11-S16.
648 Presacco, A., Simon, J. Z. and Anderson, S. (2016) Evidence of degraded representation of speech in
649 noise, in the aging midbrain and cortex. J Neurophysiol. 116(5): 2346-2355.
650 Rabang, C. F., Parthasarathy, A., Venkataraman, Y., Fisher, Z. L., Gardner, S. M. and Bartlett, E. L.
651 (2012) A computational model of inferior colliculus responses to amplitude modulated sounds in
652 young and aged rats. Front Neural Circuits 6:77.
653 Resnik, J. and Polley, D. B. (2017) Fast-spiking GABA circuit dynamics in the auditory cortex predict
654 recovery of sensory processing following peripheral nerve damage. Elife, 6.
655 Richardson, B. D., Ling, L. L., Uteshev, V. V. and Caspary, D. M. (2013) Reduced GABA(A) Receptor-
656 Mediated Tonic Inhibition in Aged Rat Auditory Thalamus. J Neurosci. 33(3): 1218-27a.
657 Rosen, S. (1992) Temporal information in speech - acoustic, auditory and linguistic aspects. Philos Trans
658 R Soc Lond B Biol Sci. 336(1278): 367-373.
659 Rosenthal, R. and Rubin, D. B. (2003) requivalent: A Simple Effect Size Indicator. Psychol Methods, 8:
660 492-496.
661 Ruggles, D., Bharadwaj, H. and Shinn-Cunningham, B. G. (2011) Normal hearing is not enough to
662 guarantee robust encoding of suprathreshold features important in everyday communication. Proc
663 Natl Acad Sci U S A. 108(37): 15516-15521.
664 Schatteman, T. A., Hughes, L. F. and Caspary, D. M. (2008) Aged-related loss of temporal processing:
665 Altered responses to amplitude modulated tones in rat dorsal cochlear nucleus. Neuroscience,
666 154(1): 329-337.
667 Schmiedt, R. A., Mills, J. H. and Boettcher, F. A. (1996) Age-related loss of activity of auditory-nerve
668 fibers, Journal of Neurophysiology, 76(4), pp. 2799-2803.
669 Sergeyenko, Y., Lall, K., Liberman, M. C. and Kujawa, S. G. (2013) Age-Related Cochlear
670 Synaptopathy: An Early-Onset Contributor to Auditory Functional Decline. J Neurosci. 33(34):
671 13686-13694.
672 Shaheen, L. A., Valero, M. D. and Liberman, M. C. (2015) Towards a Diagnosis of Cochlear Neuropathy
673 with Envelope Following Responses. J Assoc Res Otolaryngol. 16(6): 727-45
674 Spongr, V. P., Flood, D. G., Frisina, R. D. and Salvi, R. J. (1997) Quantitative measures of hair cell loss
675 in CBA and C57BL/6 mice throughout their life spans. J Acoust Soc Am. 101(6): 3546-3553.
676 Stamper, G. C. and Johnson, T. A. (2015) Auditory Function in Normal-Hearing, Noise-Exposed Human
677 Ears. Ear Hear. 36(2): 172-184.
678 Syka, J. (2010) The Fischer 344 rat as a model of presbycusis. Hear Res. 264: 70-78.

679 Takesian, A. E., Kotak V. C., Sanes D. H. (2009) Developmental Hearing loss disrupts synaptic
680 inhibition: implications for auditory processing. Future Neurol., 4(3):331-349
681 Valero, M. D., Burton, J. A., Hauser, S. N., Hackett, T. A., Ramachandran, R. and Liberman, M. C.
682 (2017) Noise-induced cochlear synaptopathy in rhesus monkeys (Macaca mulatta), Hearing
683 Research, 353, pp. 213-223.
684 Viana, L. M., O'Malley, J. T., Burgess, B. J., Jones, D. D., Oliveira, C., Santos, F., Merchant, S. N.,
685 Liberman, L. D. and Liberman, M. C. (2015) Cochlear neuropathy in human presbycusis:
686 Confocal analysis of hidden hearing loss in post-mortem tissue, Hearing Research, 327, pp. 78-88.
687 Vongpoisal, T. and Pichora-Fuller, M. K. (2007) Effect of age on F-0 difference limen and concurrent
688 vowel identification. J Speech Lang Hear Res. 50(5): 1139-1156.
689 Walton, J. P. (2010) Timing is everything: Temporal processing deficits in the aged auditory brainstem.
690 Hear Res. 264(1-2): 63-69.
691 Walton, J. P., Frisina, R. D. and O'Neill, W. E. (1998) Age-related alteration in processing of temporal
692 sound features in the auditory midbrain of the CBA mouse. J Neurosci. 18(7): 2764-2776.
693 Walton, J. P., Simon, H. and Frisina, R. D. (2002) Age-related alterations in the neural coding of envelope
694 periodicities. J Neurophysiol. 88(2): 565-578.
695 Willott, J. F., Parham, K. and Hunter, K. P. (1988a) Response properties of inferior colliculus neurons
696 in middle-aged C57bl/6J mice with presbycusis. Hear Res. 37(1): 15-27.
697 Willott, J. F., Parham, K. and Hunter, K. P. (1988b) Response properties of inferior colliculus neurons
698 in young and very old CBa/J mice. Hear Res. 37(1): 1-14.
699 Wolff, M. J., Jochim, J., Akyürek, E. G. and Stokes, M. G. (2017) Dynamic hidden states underlying
700 working-memory-guided behavior. Nat Neurosci. 20: 864-871.
701 Zhong, Z. W., Henry, K. S. and Heinz, M. G. (2014) Sensorineural hearing loss amplifies neural coding
702 of envelope information in the central auditory system of chinchillas. Hear Res. 309: 55-62.